

Anomalous Hall metals from strong disorder in class A systems on partite lattices

Eduardo V. Castro,^{1,2,*} Raphael de Gail,³ M. Pilar López-Sancho,³ and María A. H. Vozmediano³

¹*CeFEMA, Instituto Superior Técnico, Universidade de Lisboa, Av. Rovisco Pais, 1049-001 Lisboa, Portugal*

²*Beijing Computational Science Research Center, Beijing 100084, China*

³*Instituto de Ciencia de Materiales de Madrid, CSIC,*

Sor Juana Inés de la Cruz 3, Cantoblanco, E-28049 Madrid, Spain

(Dated: October 14, 2018)

Topological matter is a trending topic in condensed matter: From a fundamental point of view it has introduced new phenomena and tools, and for technological applications, it holds the promise of basic stable quantum computing. Similarly, the physics of localization by disorder, an old paradigm of obvious technological importance in the field, continues revealing surprises when new properties of matter appear. This work deals with the localization behavior of electronic systems based on partite lattices with special attention to the role of topology. We find an unexpected result from the point of view of localization properties: A robust topological metallic state characterized by a non-quantized Hall conductivity arises from strong disorder in class A (time reversal symmetry broken) insulators. The key issue is the nature of the disorder realization: selective disorder in only one sublattice in systems based on bipartite lattices. The generality of the result is based on the partite nature of most recent 2D materials as graphene or transition metal dichalcogenides, and the possibility of the physical realization of the particular disorder demonstrated in¹. An anomalous Hall metal arises also when the original clean insulator is topologically trivial.

I. INTRODUCTION

After the seminal work of P. Anderson² it was understood that in a non-interacting two dimensional electron system at zero temperature in spacial dimension $D \leq 2$ and in the thermodynamic limit, the electronic wave function will be localized by disorder. In more realistic situations the scaling theory of localization allowed a classification of the localization behavior of materials into universality classes set by symmetry and space dimensionality^{3,4} based on the Altland-Zirnbauer sets of random matrices⁵. The advent of topological insulators⁶⁻⁸ provided a new class of delocalized states, the edge states, robust under disorder provided some discrete symmetries were preserved. The symmetry classes were then adapted to include the topological features and a “tenfold way” classification was set^{9,10}.

Centering the attention on the three non-chiral symmetry classes of the original Wigner-Dyson classification

in two dimensions, we expect the following situation: All states will be localized in the orthogonal class AI (time reversal symmetry \mathcal{T} with $\mathcal{T}^2 = 1$ preserved); a mobility edge¹¹, i.e., a well defined energy separating a region of extended states from the localized states, is expected in the symplectic class AII (time reversal symmetry with $\mathcal{T}^2 = -1$ preserved). Finally, in the unitary class A (\mathcal{T} broken), extended states can remain at particular energies. Only classes A and AII support topological indices. The prototypical examples in classe A are systems showing the integer quantum Hall effect (IQHE) and anomalous quantum Hall systems, the later exemplified by the Haldane model¹². Spin Hall systems^{13,14} belong to class AII.

The interplay of topology and localization was first analyzed in the context of the robustness under disorder of the Hall conductivity quantization in the IQHE¹⁵⁻¹⁸. This is an example of a Chern insulator that belongs to symmetry class A (all discrete symmetries are broken) in the standard classification. The mechanism for localization in both topological classes A, and AII, is referred to as “levitation and annihilation”¹⁹. For moderate disorder, the states in the edges of the conduction and valence bands start to localize. As disorder increases, the gap is totally populated by localized states and the extended states carrying the Chern number shift towards one another and annihilate leading to the topological phase transition. The difference between the two classes is that, while in the symplectic class AII, a finite region of extended states with a well defined mobility edge remains until the transition takes place, there is no mobility edge in the unitary class A systems. The extended states carrying the Chern number are located at particular single energies.

We use the Haldane model¹² as a typical example of class A system based on a bipartite lattice. As it is known, depending on the parameter values, the model can represent a Chern or a trivial insulator. The main result of this work is the finding of an extended region of delocalized states with a well defined mobility edge for strong disorder in class A systems when disorder is selectively distributed in only one sublattice. Why this is surprising is because there is no mobility edge in this class. Hence our result implies that the standard classification has to be modified. Moreover the final metallic state is an anomalous Hall metal even in the case when the clean starting system is a topologically trivial insulator.

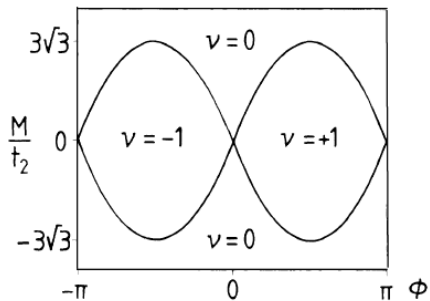


FIG. 1. Phase diagram of the Haldane model as a function of the parameters M and ϕ with $|t_2/t_1| < 1/3$. The condition $|M| = 3\sqrt{3}t_2 \sin \phi$ sets the boundary between a trivial (Chern number $\nu=0$) and a topological insulator $\nu = \pm 1$.

In addition to its fundamental interest, the physics of this work can be realized in actual material systems. Many of the 2D materials relevant for technological or fundamental physics are based on bipartite lattices. Most prominent examples like graphene and its siblings silicene, germanene, or stanene; black phosphorus, boron nitride, or transition metal dichalcogenides MX_2 ($M = \text{Mo, W}$ and $X = \text{S, Se}$) are based on the Honeycomb lattice²⁰. The experimental possibility of inducing disorder selectively in one sublattice only, has been proven in¹.

II. MODEL AND METHODS

We use the Haldane model¹² as a generic example of a Chern topological insulator. The Haldane model tight binding Hamiltonian can be written as

$$H = -t \sum_{\langle ij \rangle} c_i^\dagger c_j + -t_2 \sum_{\langle\langle ij \rangle\rangle} e^{-i\phi_{ij}} c_i^\dagger c_j \quad (1)$$

$$+ M \sum_i \eta_i c_i^\dagger c_i + \text{H.c.},$$

where $c_i = A, B$ are defined in the two triangular sublattices that form the honeycomb lattice. The first term t represents a standard real nearest neighbor hopping that links the two triangular sublattices. The next term represents a complex next nearest neighbor hopping $t_2 e^{-i\phi_{ij}}$ acting within each triangular sublattice with a phase ϕ_{ij} that has opposite signs $\phi_{ij} = \pm\phi$ in the two sublattices. This term breaks time-reversal symmetry and opens a non-trivial topological gap at the Dirac points. The last term represents a staggered potential ($\eta_i = \pm 1$). It breaks inversion symmetry and opens a trivial gap at the Dirac points. The topological transition occurs at $|M| = 3\sqrt{3}t \sin \phi$ as indicated in Fig. 1. We have done our calculations for the simplest case $\phi = \pi/2$ and a typical value $t_2 = 0.1t$. M has been set to zero except when analyzing the topologically trivial case. A physical realization of the model with optical lattices has been presented in²¹ (see also²²).

Potential (Anderson) disorder is implemented by adding to the Hamiltonian the term $\sum_{i \in A, B} \varepsilon_i c_i^\dagger c_i$, with a uniform distribution of random local energies, $\varepsilon_i \in [-W/2, W/2]$. We will discuss two cases: disorder equally or selectively distributed among the two sublattices. For selective disorder the sum runs only over one sublattice.

The Haldane model belongs to symmetry class A where the different topological phases can be characterized by a \mathbb{Z} -topological number, the Chern number ν . In the clean insulating system it can be computed from the single particle Bloch states $u_n(\mathbf{k})$ as:

$$\nu_n = \frac{1}{2\pi} \int_S \Omega_z^n(k) dS, \quad (2)$$

where the integral is over the unit cell and $\Omega_z^n(k)$ is the z component of the Berry curvature: $\Omega^n(\mathbf{k}) = \nabla_{\mathbf{k}} \wedge \mathcal{A}_n(\mathbf{k})$ defined from the Berry connection: $\mathcal{A}_n(\mathbf{k}) = \langle u_n(\mathbf{k}) | -i \nabla_{\mathbf{k}} | u_n(\mathbf{k}) \rangle$. The non trivial topology of metallic states (anomalous Hall systems) is associated to a finite, non quantized Hall conductivity that can be computed using a Kubo formula. The main technical difficulty in addressing disordered systems is the breakdown of translational symmetry which prevents working directly in momentum space. The subject being very old, many numerical and analytical tools have been worked out to deal with this oddity. Topological systems share the same problem as most topological indices are naturally defined in k space. We have used a numerical recipe based on the Kubo formula to compute the Hall conductivity in the disordered tight binding model similar to that described in²³.

The localization behavior of the system has been explored with standard tools: Level spacing statistics, and inverse participation ratio (IPR)¹⁰. A transfer matrix method²⁴ has been also used to compute the localization length and confirm the presence of a mobility edge.

III. WARMING UP: DISORDER EQUALLY DISTRIBUTED IN BOTH SUBLATTICES

We first present the case of Anderson disorder equally distributed in the two sublattices which shows the standard behavior of class A systems: extended states carrying the topological index remain at singular energies, approach each other as disorder increases (levitation) and merge (annihilation of the topological index). Figure 2 shows the spectrum for the Haldane model with Anderson disorder equally distributed over the two sublattices for a disorder strength $W = 3t$. The dots correspond to a given eigenenergy for a given disorder realization in a finite lattice with size $d = 30$. We have performed 1000 disorder realizations. Superimposed to the spectrum we show the level spacing variance as a function of energy. The variance of the level spacing variation contains information on the localization of the states at a given energy region (details can be found in the supporting information). Gaussian Unitary Ensemble (GUE) and Poisson

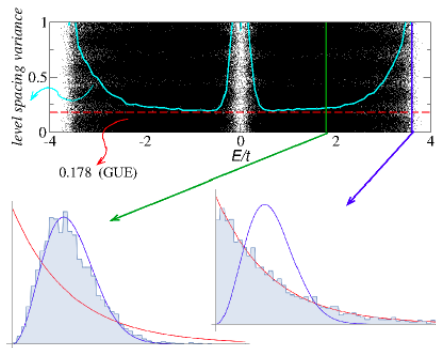


FIG. 2. Level statistics analysis for the Haldane model with Anderson disorder $W=3t$ equally distributed over the two sublattices. States are localized (Poisson distribution) all along the energy range. Extended states (GUE) are found at the two singular energies marked in the figure (green lines). This result agrees with the analysis done in Ref.²⁵.

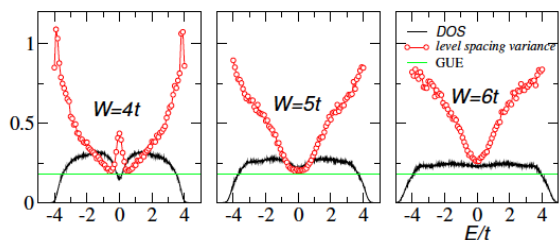


FIG. 3. Localization transition studied through level statistics for the Haldane model with Anderson disorder equally distributed over the two sublattices. The horizontal green line marks the GUE variance. The two extended states present at $W=3t$ merge around $W=5t$ and annihilate as disorder increases. All states become localized for $W > W_c \sim 5t$.

(P) ensemble statistics are associated to extended and localized states respectively. It is clear that there are two extended states, one below the gap and another one above, where the variance clearly approaches the GUE variance 0.178. These results are in perfect agreement with those presented in Ref.²⁵. In Fig. 3 we show the level statistics variance and the DOS for three different disorder strengths: $W = 4t, 5t, 6t$. Levitation and annihilation is clearly operative, and the critical disorder for localization is in good agreement with that obtained in ref.²⁶ for the topological transition, $4t < W_c < 5t$.

IV. MAIN RESULTS

A. Disorder selectively distributed in only one sublattice: Topological model

The first unexpected result obtained is that, for selectively distributed disorder in only one sublattice, the class A system ends up in a robust metallic state where

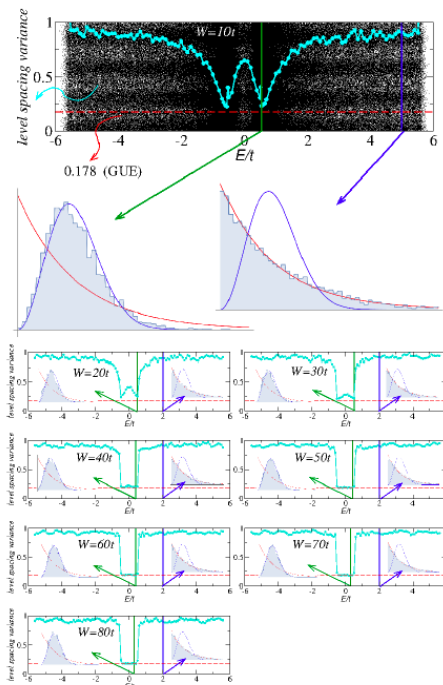


FIG. 4. Level statistics analysis for the Haldane model with Anderson disorder selectively distributed over one sublattice. The red dotted horizontal line marks the variance of the GUE associated to the presence of extended states. As disorder increases, the singular energies where extended states were located at moderate disorder strength $W/t = 20 - 30$, evolve to a full extended region of delocalized states with a well defined mobility edge.

the extended states are separated from the localized states at the band edges by a well defined mobility edge. Figure 4 shows a level spacing statistic analysis of the system for increasing disorder strength. What we see in the figure is the statistics associated to two characteristic energies in the spectrum: one at the edge (blue line) where states start to localize first when disorder is introduced, and one at the middle of the band (green line) where extended states are expected to persist up to higher disorder strength. The red dotted horizontal line marks the variance of the GUE associated to the presence of extended states. We see that, as disorder increases, the singular energies where extended states were located at moderate disorder strength $W/t = 20 - 30$, evolve to a full extended region of delocalized states with a well defined mobility edge. Fig. 5 shows that the extended region of delocalized states is a robust feature that persists up to a disorder strength of $W=200t$. We have also set up a calculation of the localization length via a transfer matrix method to confirm the presence of the mobility edge.

The topological nature of the metallic state is reflected in the calculation of the Hall conductivity shown in Fig. 6. In our previous publication²⁶ we showed that the Chern insulator suffered a topological transition to a trivial state at a critical disorder strength around $W_c \sim 50t$.

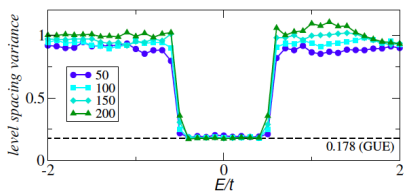


FIG. 5. Level spacing variation for increasing disorder strengths W/t in the selectively distributed disorder case. The middle region has the same variance as that of GUE and corresponds to extended states. Even though the transition is becoming sharper, the region is not shrinking. This is a clear evidence for the existence of an extended region of delocalized states. A mobility edge in the center of the band has emerged from the singular, isolated energies by increasing disorder.

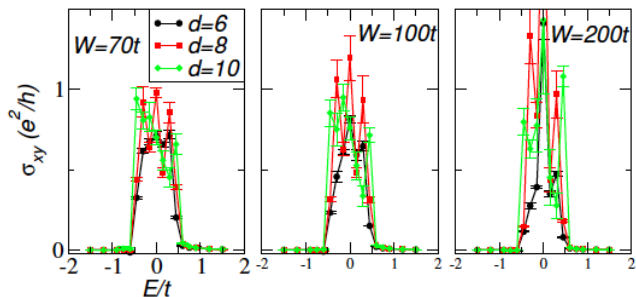


FIG. 6. Hall conductivity of the resulting metallic state emerging from the Chern insulator for disorder strengths above the critical value for the topological transition. The conductivity is not quantized and depends on the chemical potential. Despite the big numerical error bars a finite non-zero value can be granted.

What we see here is the further evolution to an anomalous Hall metal when disorder is further increased and the metallic state is well established. The panels in Fig. 6 show that the Hall conductivity stays finite in the metallic region for $W > W_c$. The different curves correspond to different sizes of the system. We see that for increasing system sizes σ_{xy} is not decreasing what proves that we are not dealing with a finite size effect. Despite the large numerical error bars (bigger for smaller sizes), a finite conductivity can be granted.

B. Disorder selectively distributed in only one sublattice: Topologically trivial case

The second unexpected result is obtained when analyzing the trivial case. As it was mentioned when describing the Haldane model, the parameters can be tuned to describe a trivial insulator for values of the staggered potential $|M| > 3\sqrt{3}t_2 \sin \phi$. In order to ascertain the possible role of topology in the development of the metallic phase, we have analyzed the localization behavior of the trivial case with generic values of the parameters chosen so that T is still broken but the original insulator has a trivial

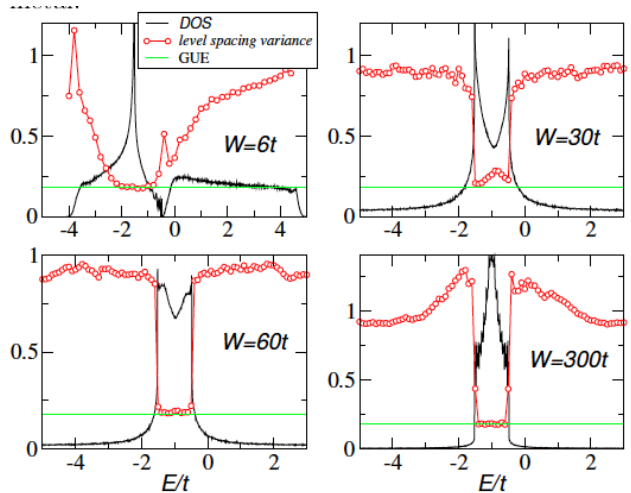


FIG. 7. Level spacing variation for the disordered trivial insulator in the selectively distributed disorder case. The results are very similar to these in the topological case in Fig. 5.

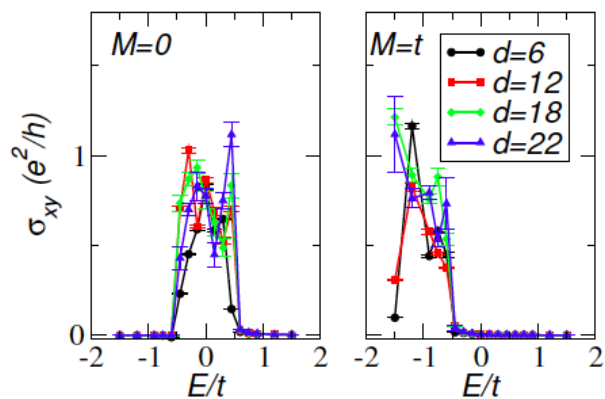


FIG. 8. A comparison of the Hall conductivity of the resulting metallic state emerging from the topological (left hand side) and trivial insulator (right hand side). A finite Hall conductivity is obtained in both cases.

gap with zero Chern number. The localization properties are shown in fig. 7. The final state is metallic with a well defined mobility edge. The topological nature of the final state is reflected in the Hall conductivity shown in Fig. 8. We compare the topological $M = 0$ case with the trivial $|M| > 3\sqrt{3}t_2 \sin \phi$ for $t_2/t = 0.1e^{i\pi/2}$. We have used larger system sizes, and higher number of disorder realizations; 105, 105, 104, and 5000 disorder realizations, respectively for $d = 6, 12, 18,$ and 22 . Note that σ_{xy} is finite only in the energy region where states have a larger amplitude in the non-disorder sublattice. These findings agree well with the results for the level spacing variance discussed above.

V. UNDERSTANDING WHAT IS GOING ON: SIDE QUESTIONS.

This work rises a number of additional questions. We have addressed some of them, others remain open.

For simplicity, a purely imaginary value of the t_2 parameter $t_2 = i0.1t$ has been used through the work ($\phi = \pi/2$). This choice induces an accidental particle-hole symmetry to the system that technically belongs to class D. We have performed some additional calculations with a non-zero real part for t_2 to ensure that we are discussing class A physics and found no qualitative differences. It could be thought that, since disorder affects only one sublattice, the final metallic state coincides with the trivial metal of the triangular lattice. The result of the Hall conductivity makes obvious that this is not so. We have performed some calculations of partial IPR and saw that the wave function of extended states has always some weight in the disordered sublattice. It is interesting to note that this is so also in the case of vacancy disorder when the disordered sublattice is depleted.

Irrespective of the topological character of the clean system, the final state in the class A analyzed is a T broken disordered metal with finite Hall conductivity. Our results show that, while a topological insulator can be become trivial by an appropriate tuning of the parameters as happens in the Haldane model, the anomalous Hall metal is a very robust and a stable phase for T broken metals in the absence of an external magnetic field.

As we mentioned above, even when for the highest values of disorder, the disordered sublattice is never decoupled from the ordered one. The physics that we observe all along the work is that of the disordered Honeycomb lattice, as proven by the fact that the extended states found in the extreme disorder case have a non zero weight in the disordered sublattice. Even though the weight in the disordered sublattice is orders of magnitude smaller than in the clean sublattice, the two sublattices do not "decouple". This explains the metallic nature of the final state: An electron in the disordered sublattice can

propagate to a very long distant site by hopping to the clean sublattice, propagate there, and hop back. The probability of the process is suppressed to be of order αt^2 but it is never zero. This also explains why the final metallic state is a topological metal since the anomalous Hall effect is due to the interband matrix elements of the current operators²⁷.

The different behavior of IQHE and anomalous Hall metals under disorder has been examined in refs.^{28,29}. The properties of disordered topological metals arising from clean topological insulators have been analyzed in ref. 30. The metallicity of the final state seems to be at odds with the non-linear sigma model results^{10,31} so it would be very interesting to implement the selective disorder case in this approach.

The physics described in this work can be realized in topological materials based on other more complicated partite lattices³². The results presented in this work are conceptually important, although we recognize that to implement the selectively distributed disorder might be a hard task. To this respect, we note that experiments have been done in graphene where defects are located selectively in one sublattice to check the magnetic properties of the system¹. Artificial³³ or optical lattices²¹ are other possibilities to realize this physics.

ACKNOWLEDGMENTS

We gratefully acknowledge useful conversations with Alberto Cortijo, Belén Valenzuela, Fernando de Juan, Adolfo G. Grushin, and J. A. Vergés. EC acknowledges the financial support of FCT-Portugal through grant No. EXPL/FIS-NAN/1728/2013. This research was supported in part by the Spanish MECD grants FIS2014-57432-P, the European Union structural funds and the Comunidad de Madrid MAD2D-CM Program (S2013/MIT-3007), the European Union Seventh Framework Programme under grant agreement no. 604391 Graphene Flagship FPA2012-32828.

* eduardo.castro@tecnico.ulisboa.pt

¹ Ugeda, M. M., Brihuega, I., Guinea, F. & Gómez-Rodríguez, J. M. Missing atom as a source of carbon magnetism. *Phys. Rev. Lett.* **104**, 096804 (2010).

² Anderson, P. W. Absence of diffusion in certain random lattices. *Phys. Rev.* **109**, 1492–1505 (1958).

³ Abrahams, E., Anderson, P. W., Licciardello, D. C. & Ramakrishnan, T. W. Scaling theory of localization: Absence of quantum diffusion in two dimensions. *Phys. Rev. Lett.* **42**, 673 (1979).

⁴ Anderson, P. W., Thouless, D. J., Abrahams, E. & Fisher, D. S. New method for a scaling theory of localization. *Phys. Rev. B* **22**, 3519–3526 (1980).

⁵ Altland, A. & Zirnbauer, M. R. Nonstandard symmetry classes in mesoscopic normal-superconducting hybrid structures. *Phys. Rev. B* **55**, 1142 (1997).

⁶ Bernevig, B. A., Hughes, T. L. & Zhang, S. Quantum spin hall effect and topological phase transition in hgte quantum wells. *Science* **314**, 1757 (2006).

⁷ Hasan, M. Z. & Kane, C. L. Topological insulators. *Rev. Mod. Phys.* **82**, 3045 (2010).

⁸ Qi, X. & Zhang, S. Topological insulators and superconductors. *Rev. Mod. Phys.* **83**, 1057 (2011).

⁹ Schnyder, A. P., Ryu, S., Furusaki, A. & Ludwig, A. W. W. Classification of topological insulators and superconductors in three spatial dimensions. *Phys. Rev. B* **78**, 195125 (2008).

¹⁰ Evers, F. & Mirlin, A. D. Anderson transitions. *Rev. Mod. Phys.* **80**, 1355 (2008).

¹¹ Lee, P. A. & Ramakrishnan, T. V. Disordered electronic systems. *Rev. Mod. Phys.* **57**, 287–337 (1985).

¹² Haldane, F. D. M. Model for a quantum hall effect without

- landau levels: Condensed-matter realization of the parity anomaly. *Phys. Rev. Lett.* **61**, 2015–2018 (1988).
- ¹³ Kane, C. & Mele, E. Quantum spin hall effect in graphene. *Phys. Rev. Lett.* **95**, 226801 (2005).
- ¹⁴ Kane, C. & Mele, E. Z₂ topological order and the quantum spin hall effect. *Phys. Rev. Lett.* **95**, 146802 (2005).
- ¹⁵ Pruisken, A. The integral quantum hall effect: Shortcomings of conventional localization theory. *Nucl. Phys. B* **295**, 253 (1988).
- ¹⁶ Pruisken, A. M. M. Universal singularities in the integral quantum hall effect. *Phys. Rev. Lett.* **61**, 1297 (1988).
- ¹⁷ Chalker, J. T. & Coddington, P. D. Percolation, quantum tunnelling and the integer hall effect. *J. Phys. C: Solid State Phys.* **21**, 2665 (1988).
- ¹⁸ Ludwig, A. W. W., Fisher, M. P. A., Shankar, R. & Grinstein, G. Integer quantum hall transition: An alternative approach and exact results. *Phys. Rev. B* **50**, 7526 (1994).
- ¹⁹ Onoda, M., Avishai, Y. & Nagaosa, N. Localization in a quantum spin hall system. *Phys. Rev. Lett.* **98**, 076802 (2007).
- ²⁰ Gibney, E. The super materials that could trump graphene. *Nature* **522**, 274 (2012).
- ²¹ Jotzu, G. *et al.* Experimental realization of the topological haldane model with ultracold fermions. *Nature* **515**, 237 (2014).
- ²² Wright, A. R. Realising haldane’s vision for a chern insulator in buckled lattices. *Nature Scientific Reports* **3**, 2736 (2013).
- ²³ Crepieux, A. & Bruno, P. Theory of the anomalous hall effect from the kubo formula and the dirac equation. *Phys. Rev. B* **64**, 014416 (2001).
- ²⁴ E. Abrahams, editor. *50 years of anderson localization* (World Scientific, Singapore, 2010).
- ²⁵ Prodan, E. Disordered topological insulators: a non-commutative geometry perspective. *Journal of Physics A: Mathematical and Theoretical* **44**, 113001 (2011).
- ²⁶ Castro, E. V., López-Sancho, M. P. & Vozmediano, M. A. H. Anderson localization and topological transition in chern insulators. *Phys. Rev. B* **92**, 085410 (2015).
- ²⁷ Karplus, R. & Luttinger, J. M. Hall effect in ferromagnetics. *Phys. Rev.* **95**, 1154 (1954).
- ²⁸ Onoda, M. & Nagaosa, N. Topological nature of anomalous hall effect in ferromagnets. *J. Phys. Soc. Japan* **71**, 19 (2002).
- ²⁹ Onoda, M. & Nagaosa, N. Quantized anomalous hall effect in two-dimensional ferromagnets - quantum hall effect from metal -. *Phys. Rev. Lett.* **90**, 206601 (2003).
- ³⁰ Meyer, J. S. & Refael, G. Disordered topological metals. *Phys. Rev. B* **87**, 104202 (2013).
- ³¹ Morimoto, T., Furusaki, A. & Mudry, C. Anderson localization and the topology of classifying spaces. *Phys. Rev. B* **91**, 235111 (2015).
- ³² Xu, G., Lian, B. & Zhang, S.-C. Intrinsic quantum anomalous hall effect in the kagome lattice $cs_2limn_3f_{12}$. *Phys. Rev. Lett.* **115**, 186802 (2015).
- ³³ Gomes, K. K., Mar, W., Ko, W., Guinea, F. & Manoharan, H. C. Designer dirac fermions and topological phases in molecular graphene. *Nature* **483**, 306 (2012).